New insights into cadherin function in epidermal sheet formation and maintenance of tissue integrity

Christopher L. Tinkle, H. Amalia Pasolli, Nicole Stokes, and Elaine Fuchs*

Laboratory of Mammalian Cell Biology and Development, Howard Hughes Medical Institute, The Rockefeller University, New York, NY 10065

Contributed by Elaine Fuchs, August 3, 2008 (sent for review June 18, 2008)

Co-expression and gene linkage have hampered elucidating the physiological relevance of cadherins in mammalian tissues. Here, we combine conditional gene ablation and transgenic RNA interference to uncover new roles for E- and P-cadherins in epidermal sheet formation *in vitro* and maintenance of epidermal integrity *in vivo*. By devising skin-specific RNAi technology, we demonstrate that cadherin inhibition *in vivo* impairs junction formation and intercellular adhesion and increases apoptosis. These defects compromise epidermal barrier function and tissue integrity. *In vitro*, with only E-cadherin missing, epidermal sheet formation is delayed, but when both cadherins are suppressed, defects extend to adherens junctions, desmosomes, tight junctions and cortical actin dynamics. Using different rescue strategies, we show that cadherin level rather than subtype is critical. Finally, by comparing conditional loss-of-function studies of epidermal catenins and cadherins, we dissect cadherin-dependent and independent roles of adherens junction components in tissue physiology.

adherens junctions | epidermis | intercellular adhesion | tissue specific shRNA delivery

Adherens junctions (AJs) function in the dynamic regulation of intercellular adhesion (1). The epithelial AJ transmembrane core is composed of E-cadherin (Ecad), whose ectodomain binds Ca^{2+} to mediate transcadherin interactions between neighboring cells (2, 3). Its intracellular domain binds directly to p120-catenin and β-catenin, which in turn binds to α-catenin. Together, catenins regulate cadherin stability and coordinate associated actin dynamics to ensure efficient cell adhesion (1, 4).

E-cadherin, *P-cadherin*, *α-catenin*, *p120-catenin* and *β-catenin* have all been conditionally targeted for ablation in mouse epidermis, making it an excellent system to probe the physiological importance of AJ components (5–11). Given the well-established connection between cadherin/catenin mutations and cancers, it was not initially surprising to find that loss of AJ components predisposed skin to cancers. Curiously, however, obvious disruptions of intercellular adhesion are not always among the most striking defects arising from catenin deficiencies in skin (5, 6, 8, 12, 13). Thus, although loss of α-catenin disrupts epidermal adhesion, the hyperproliferation and inflammation associated with this loss do not rely upon the severing of junctions, but rather on perturbations in Ras-MAPK and NF-κB signaling. Moreover, epidermal adhesion is seemingly unaltered when β-catenin or p120-catenin is absent, and instead, respective defects in Wnt signaling and inflammation prevail.

Ascertaining classical cadherin function(s) in epidermis has been complicated by the up-regulation of P-cadherin (Pcad) in the basal layer when Ecad is absent, the tight linkage of *Ecad* and *Pcad* genes, and the presence of cadherin-catenin complexes at cell borders in the other AJ mutant mouse models (10, 11). Using a combined knockout/RNAi strategy, we have now overcome these difficulties and uncovered defects not present in single loss of function mutations for any of the AJ components. Our studies reveal new insights into the functional significance of Ecad and Pcad in the formation of cell adhesion complexes in keratinocytes *in vitro* and in maintenance of epidermal integrity *in vivo*.

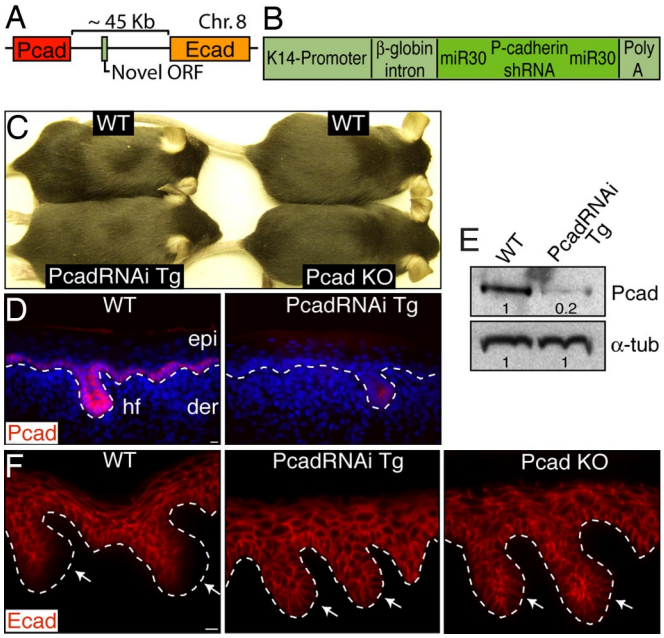

Fig. 1. Generation of *Pcad* RNAi transgenic mice. (*A*) Schematic of the *Pcad* and *Ecad* chromosomal locus. (*B*) The *K14-Pcad* RNAi construct used to generate transgenic (Tg) mice. (*C*) Images of WT and *PcadRNAi* Tg littermates and WT and *Pcad* KO littermate adult mice. (*D* and *F*) Newborn (P0) tail skins of indicated mice were processed for indirect immunofluorescence with indicated Abs. Arrows denote downregulation of Ecad at sites of HF downgrowth in WT, but not *Pcad* KO or *PcadRNAi* Tg mice. (*E*) Immunoblot analyses of P0 epidermal lysates with indicated Abs; α-tub (α-tubulin). epi, epidermis; der, dermis; hf, hair follicle. Dotted lines represent junction between epidermis and dermis. (Scale bars, 10 μm.)

Results

Generation of Cadherin-Deficient Epidermis in Mice. *Ecad* and *Pcad* genes are tightly (approximately 45 kb) linked on chromosome 8 (14) and separated by a predicted ORF of unknown function (Fig. 1*A*). Since this precludes conventional strategies, we first engineered transgenic (Tg) mice expressing *P-cadherin* short hairpin RNA (shRNA) driven by the epidermal *keratin 14* (*K14*) promoter (Fig. 1*B*). Three independent *PcadRNAi* Tg lines were established, each with similar levels of *Pcad* knockdown.

PcadRNAi Tg mice were viable and displayed no obvious skin phenotype even though epidermal P-cadherin was significantly

Author contributions: C.L.T., H.A.P., and E.F. designed research; C.L.T., H.A.P., and N.S. performed research; C.L.T., H.A.P., and E.F. analyzed data; and C.L.T. and E.F. wrote the paper.

The authors declare no conflict of interest.

Freely available online through the PNAS open access option.

*To whom correspondence should be addressed: E-mail: fuchslb@rockefeller.edu.

See Commentary on page 15225.

This article contains supporting information online at www.pnas.org/cgi/content/full/0807374105/DCSupplemental.

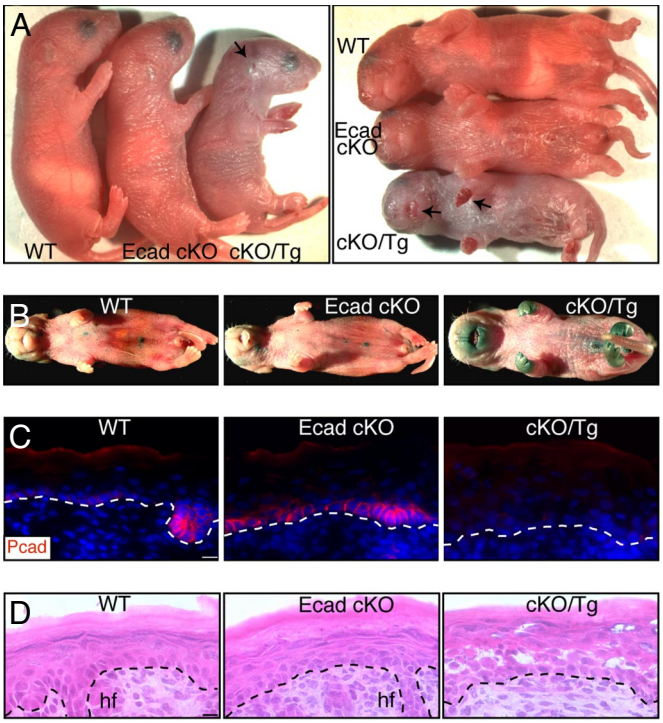

Fig. 2. Inhibition of classical cadherins in mouse epidermis results in cell dissociation, blistering skin lesions, and defective epidermal barrier. *PcadRNAi* Tg and *K14-Cre*/*Ecad* cKO mice were bred to generate P0 mice WT or conditionally null for the *Ecad* allele and either negative (*Ecad* cKO) or positive (cKO/Tg) for the *PcadRNAi* transgene. Arrows in *A* denote blistered skin lesions, seen only in cKO/Tg mice. Barrier function analyses in *B* assessed by exclusion of an XGAL-containing solution. Arrows indicate areas, found only in cKO/Tg mice, where skin barrier function is disrupted and endogenous β-galactosidase converts dye to blue. Immunofluorescence in *C* shows absence of P-cadherin in cKO/Tg backskin epidermis (epidermal Ecad is completely absent in *Ecad* cKO mice) (10). H&E staining in *D* reveals that such regions lacking both cadherins exhibit gross perturbations in tissue integrity.

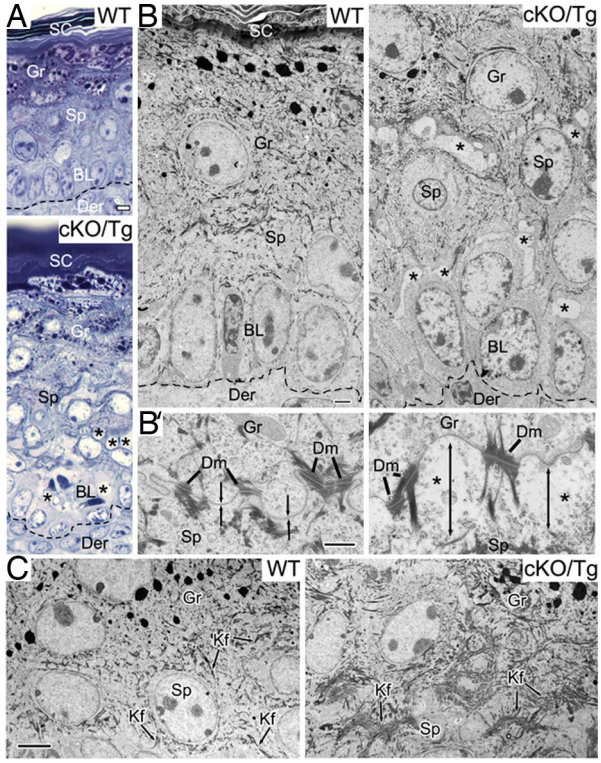

Fig. 3. Ultrastructural abnormalities in cadherin-deficient epidermis. (*A*) 0.8 μm semithin sections of P0 backskins were stained with toluidine blue. Asterisks denote intercellular gaps between keratinocytes of cKO/Tg epidermis. Also note epidermal hyperthickening and marked disorganization and altered cuboidal morphology of basal cells in cKO/Tg skin. (*B* and *C*) Transmission electron microscopy. Asterisks in (*B* and *B′*) and double arrows in (*B′*) denote intercellular gaps. Despite gaps and signs of cellular degeneration, double membranes appear to persist between cKO/Tg keratinocytes. Note also that desmosomes (Dm), which were not reduced in number, appear to be intact even in areas where intercellular gaps occurred (*B′*). Region in *C* contrasts the normal desmosome-keratin filament network of suprabasal cells of WT epidermis versus the irregular aggregates of keratin filaments (Kf) that were frequently observed in cKO/Tg epidermis. Such alterations in keratin organization frequently reflect defects in mechanical integrity. Additional abbreviations: BL (basal layer); Sp (spinous layer); Gr (granular layer); SC (stratum corneum). Dotted lines in *A* and *B* represent junction between epidermis and dermis. (Scale bars: *A*, 5 μm (*A*); *B*, 2 μm; *B′*, 500 nm; *C*, 5 μm.)

reduced (Fig. 1*C–E*). Histologically and biochemically, Tg skin appeared normal except that Ecad was not downregulated at sites of hair follicle (HF) downgrowth (15, 16) (Fig. 1*F*). This alteration was also seen in mice lacking Pcad (*Pcad* KO) (7), underscoring the specificity of the *PcadRNAi* transgene *in vivo*. Each of these *PcadRNAi* Tg lines were then mated to our *Ecad* conditional knockout (cKO) mice (10) to generate mice deficient for epidermal cadherins.

Novel Phenotypic and Morphological Perturbations in the Absence of Epidermal Cadherins. *K14-Cre*/*Ecad*(fl/fl)/*K14-PcadRNAi* (cKO/Tg) mice displayed dramatic phenotypic abnormalities which distinguished them from their single loss-of-function counterparts (Fig. 2*A*). cKO/Tg mice were atypically small and died 1–2 h after birth. Their skin was shiny like that of *Ecad* cKO mice, but it was also taut and inflexible and showed considerable ventral flaking. Additionally, their skin blistered on the paws and around the mouth, umbilicus, and tail (arrows). Moreover, newborn (P0) cKO/Tg pups aberrantly adsorbed dye through their paws, facial skin, ear buds and lower belly, reflective of a defective epidermal barrier (Fig. 2*B*).

Pcad was not detected over large regions of cKO/Tg skin (Fig. 2*C*). Despite germline transmission, and for reasons unclear, F1 pups from different Tg lines displayed patches of Pcad(+) skin ($\approx$5% of total backskin, data not shown) providing an internal control for our analyses. Areas devoid of cadherins displayed severe histological abnormalities not evident in *Ecad* cKO epidermis or in cKO/Tg regions lacking only Ecad. HFs were fewer and were either Pcad(+) or severely stunted (see below). Most notable was a loss of epidermal integrity accompanied by an apparent hyperthickening within areas lacking both cadherins (Fig. 2*D*).

Ultrastructurally, distortions in cellular morphology were sufficiently severe to account for the observed epidermal hyperthickening [Fig. 3*A* and supporting information (SI) Fig. S1*A*]. Notably, the typical columnar orientation of cells within the basal layer was largely lost in cadherin-deficient epidermis as was the flattened squamous morphology typical of WT suprabasal cells. Although most intercellular membranes appeared to be sealed, focal gaps compromised the continuity of the epithelial sheets (Fig. 3 *A* and *B*).

Interestingly, desmosomes (Dms) still formed in normal numbers (Fig. 3*B′* and data not shown). Intercellular gaps seemed to arise not from splits within Dms, but rather from degeneration of one of the two neighboring cells (asterisks in Fig. 3*B′*). Such perturbations increased Dm density in some areas and decreased it in others, suggestive of a collapse in cellular integrity. Dissociated suprabasal cells occasionally displayed condensed nuclei,

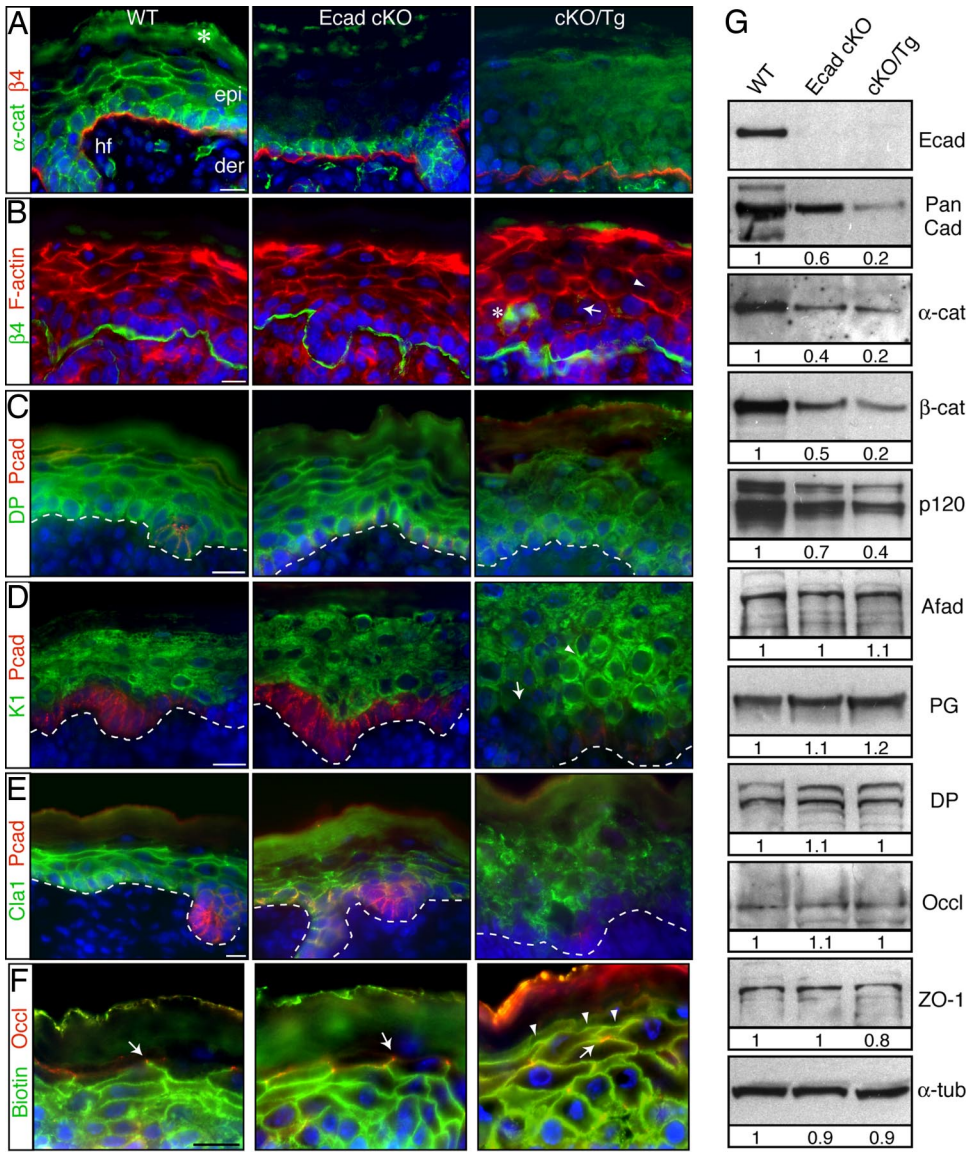

Fig. 4. Perturbations in intercellular junctions, cytoskeleton organization, and tight junction function in epidermis lacking E- and P-cad. (*A–F*) P0 skins from tail (*D*) and back (all others) were processed for fluorescence microscopy with indicated Abs or TRITC-Phalloidin (actin, red). Additional Ab abbreviations: α-cat (α-catenin); β4 (β4 integrin), hemidesmosomal component restricted to the base of the basal layer; DP (desmoplakin); K1 (keratin 1), component of suprabasal IF network; ClaI (claudin 1); Occl (occludin). Asterisk in *A* denotes nonspecific 2^0Ab staining of cornified layer. Abnormalities unique to cKO/Tg skin are denoted by: Arrows in *B* and *D*, gaps between basal and suprabasal cells; arrowhead in *B*, absence of cortical actin network between two suprabasal keratinocytes; asterisk in *B*, expansion of β4 integrin localization into spinous layers (cornified cell staining is nonspecific as per above); arrowhead in *D*, non-uniform staining patterns of keratin in some suprabasal keratinocytes. (*F*) Inside-out permeability assessed by monitoring impedance to biotin flow at TJs in granular layer. Arrows indicate occludin-based TJs. Arrowheads denote biotin flow past TJs in cKO/Tg epidermis only. (*G*) Immunoblot analysis of total P0 epidermal lysates with indicated Abs; Pan Cad (pan cadherin); β-cat (β-catenin); p120 (p120-catenin); Afad (afadin); PG (plakoglobin). (Scale bars: 10 μm.)

indicative of apoptosis (data not shown). Finally, suprabasal keratin intermediate filament (IF) organization was perturbed (Fig. 3*C* and Fig. S1*B*). Overall, these features suggested an increased mechanical fragility within cKO/Tg epidermis.

Global Junctional Perturbations Without Epidermal Cadherins. Classical cadherins appeared to be effectively targeted in cKO/Tg epidermis, since all other AJ components failed to localize to cell borders (Fig. 4 *A* and *G* and Fig. S2 *A* and *B*). Actin organization was also aberrant particularly at sites of suprabasal cell-cell contacts (Fig. 4*B*). The disorganized and often discontinuous cortical actin belts could explain why suprabasal cells failed to adopt the flattened squamous shape of their WT counterparts. Signs of actin disorganization were also evident in the basal layer, as reflected by altered cellular organization, and by discontinuous basal and atypical spinous layer immunolocalization of hemidesmosomal integrin β4 (Fig. 4*B*).

Dm cadherins (desmocollin-2 and desmoglein) and the keratin IF-Dm linker protein (desmoplakin) still localized to cell borders, and total levels of Dm proteins were unchanged (Fig. 4*G* and data not shown). Consistent with our ultrastructural findings, however, immunolabeling was discontinuous (Fig. 4*C* and Fig. S2 *C* and *D*). Similarly, suprabasal keratin 1 (K1) immunolocalization was often perinuclear (Fig. 4*D*), reflective of the abnormal intracellular aggregates of keratin IFs observed ultrastructurally.

Cadherin deficiency also resulted in defects in intercellular border localization but not overall levels of tight junction (TJ) proteins claudin 1, occludin, and ZO-1 (Fig. 4 *E* and *G* and

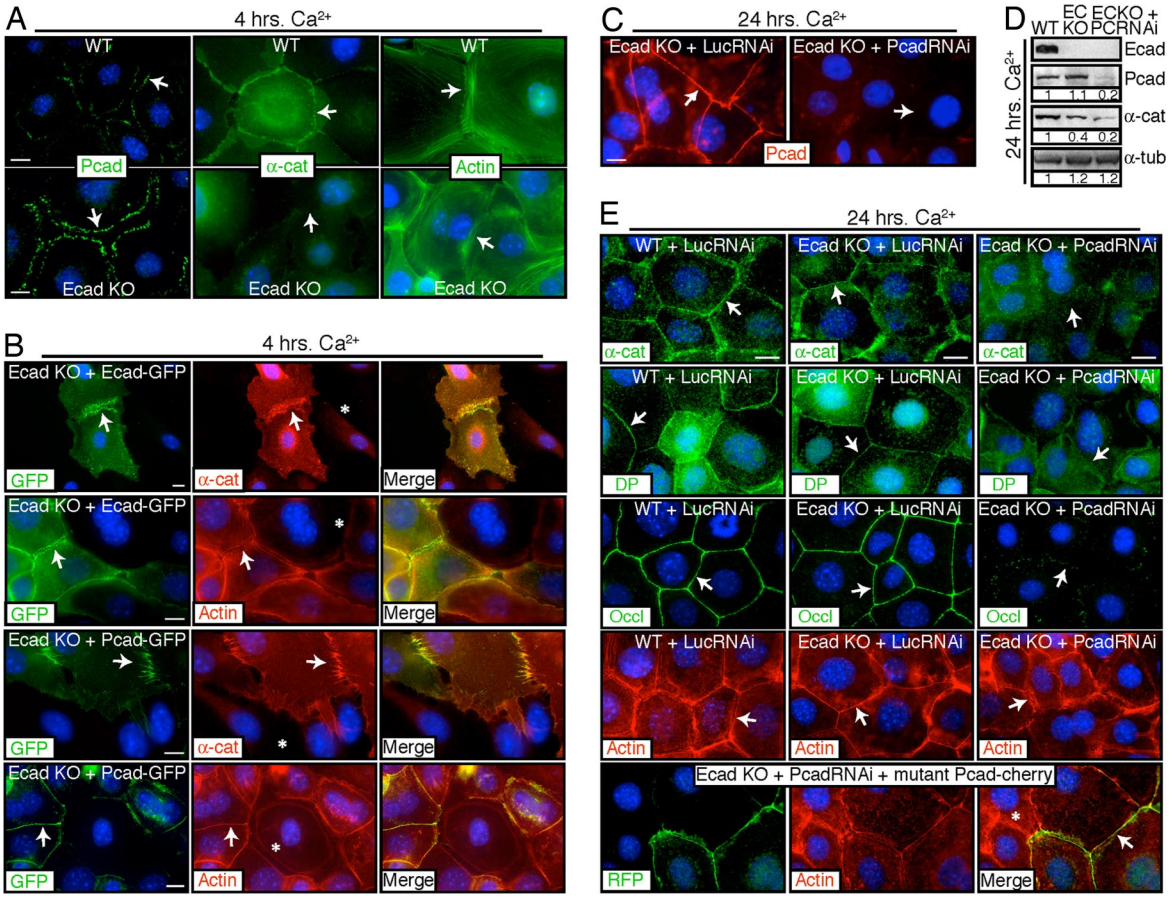

Fig. 5. Overall cadherin level governs epidermal sheet formation *in vitro*. (*A–E*) Confluent monolayers of WT and *Ecad* KO primary mouse keratinocytes (1^0MKs) alone or stably expressing indicated constructs were shifted from low (0.05 mM) to high (1.5 mM) Ca^{2+} media for indicated times before processing for fluorescence microscopy with Abs or Alexa 647-phalloidin (actin, red) as indicated and immunoblot analysis of total lysates (*D*). Actin in *A* and *B* represents epifluorescence from K14-GFPactin (28) 1^0MKs WT or null for *Ecad*. Arrows in all images indicate sites of cell-cell interactions. (*A*) Despite increased Pcad at puncta, *Ecad* KO 1^0MKs display delayed kinetics of catenin localization and actin organization. (*B*) Expression of either Ecad-GFP or Pcad-GFP rescues the early delay in epidermal sheet formation in *Ecad* KO 1^0MKs. Asterisks denote sites of interactions between *Ecad* KO cells that do not express cadherin-GFP. (*C* and *D*) Immunofluoresence and immunoblot analysis of *PcadRNAi in vitro*. (*E*) Inhibition of Ecad and Pcad blocks epidermal sheet formation *in vitro* and this is rescued by expression of silencing resistant Pcad-cherry fusion protein. Anti-RFP antibody was used to detect mutant Pcad protein. Asterisks specifically indicate sites of interactions between *Ecad* KO + *Pcad*RNAi cells lacking rescue construct. (Scale bars: 10 μm.)

Fig. S2 *E* and *F*). TJs appeared to be functionally compromised, since upward biotin flow was not blocked at the granular layer (Fig. 4*F*), i.e., where TJs are normally assembled (17). Although a TJ defect was noted in a different strain of *Ecad* cKO mice (11), the epidermis from our *Ecad* cKO strain showed biotin flow restriction. Strain-specific differences aside, the striking differences in single versus double cadherin inhibition underscored the importance of cadherins in overall formation and/or stability of TJs.

Recent studies suggest that cadherin-based cell adhesion may function not only in Dm and TJ assembly but also in epithelial cell polarity (18). Interestingly, cadherin-deficient epidermis displayed defective localization of Par3, aPKC, and Scribble (Fig. S3 *A–C*). By contrast, loss of Ecad alone did not alter Par3 (11) or Scribble distribution (Fig. S3 *A* and *C*). While our current understanding of polarity-regulating complexes in stratified epithelia is limited, these findings suggest that cadherins are required for their proper localization. These findings lend physiological relevance to *in vitro* connections previously identified between AJs and polarity proteins of the Scribble complex (19).

Additional Insights from *in Vitro* Studies. The defects in intercellular junction assembly and actin dynamics were further characterized *in vitro* by infecting *Ecad* cKO primary mouse keratinocytes (1^0MK) with a retrovirus expressing short hairpin (sh) RNAs against *Pcad* (Fig. 5 *C* and *D*). Loss of Ecad alone delayed Ca^{+2}-induced AJ formation and assembly of 1^0MK into a continuous sheet (Fig. 5*A* and Fig. S4*A*). However, without Pcad and Ecad, catenins weren't recruited to cell contacts and sheets failed to form even after 24 h exposure to high Ca^{2+} (Fig. 5*E* and Fig. S4*B*). Additionally, F-actin was not organized properly and Dm and TJ constituents no longer localized to cell borders (Fig. 5*E*). Each of these defects was rescued by a *P-cadherin-cherry* mRNA that was silencing-resistant, underscoring the specificity of the shRNA (Fig. 5*E* and Fig. S4 *C* and *D*).

Based upon these data, we conclude that sustained junctional defects and failure in sheet formation are a consequence of loss of cadherin function. Moreover, two lines of evidence suggested that the delay in epidermal sheet formation observed with *Ecad* KO 1^0MK was due to a reduction in overall cadherin level rather than Ecad loss *per se*. First, endogenous Pcad levels rose steadily in both WT and *Ecad* KO 1^0MK following Ca^{+2} exposure, and this correlated with sheet assembly (Fig. S4 *F* and *E*). Second, Ecad and Pcad GFP fusion proteins both rescued the delayed kinetics of *Ecad* KO 1^0MKs (Fig. 5*B*).

Dissecting AJ-Dependent vs. AJ-Independent Defects. The adhesion and junctional defects associated with cadherin loss resembled

those of α-catenin cKO skin (20). Additionally, although we previously noted mild alterations in Ecad cKO-associated epidermal differentiation (10), such defects were not detected in the Ecad cKO or cadherin-deficient strains used here (Fig. S3 *D–F*) nor in α-catenin cKO mice (6).

By contrast, in both cadherin and α-catenin deficient epidermis, apoptosis was increased (Fig. 6 *A–D*), a finding also documented in Ecad-deficient mammary gland (21). Cells positive for TUNEL and activated caspase 3 were most often suprabasal and dissociated from neighbors (Fig. 6 *A* and *B*; Fig. S5 *A* and *B*). Since apoptosis was not enhanced in desmoplakin cKO epidermis (Fig. S5*B*) (22), the effects appeared to be specific to AJ formation rather than intercellular adhesion *per se*.

The hyperthickened epidermis associated with cadherin loss suggested that the skin might be hyperproliferative as well. Surprisingly, however, incorporation of the thymidine analog BrdU revealed no significant differences in the number or basal location of epidermal cells actively in S-phase (Fig. 6 *E* and *F*). Similarly, immunofluorescence with the mitosis marker phospho-histone H3 revealed no differences in basal location or numbers of positive cells, and no changes were detected in activated MAPK levels (Fig. S5*C* and Fig. 6*G*). Although keratin 6 was induced (Fig. S5*D*), this is only a broad indicator of perturbed epidermal biology and not hyperproliferation *per se* (23).

The lack of proliferative defects in cadherin-deficient skin contrasted with α-*catenin* and/or *p120-catenin* cKO skins (5, 6). An additional perturbation arising from α-*catenin* and *p*-120 catenin loss (5, 12) was a striking inflammatory cell infiltrate and epidermal NF-κB activation. Surprisingly, however, neither inflammatory cell recruitment nor NF-κB activation were features of cadherin-deficient epidermis (Fig. S5 *E* and *F* and Fig. 6*H*).

Discussion

Conditional targeting of a specific shRNA *in vivo* represents a technological advance that should be broadly applicable in the future. By removing cadherins *in vivo*, subsequent to intercellular junction formation, we have uncovered a dependency of TJs on classical cadherins that has not been evident from *in vitro* studies (24, 25). In addition, even though Dms formed, the Dm-keratin IF network appeared no longer able to provide mechanical integrity. Interestingly, a collapse in epidermal architecture rather than a disruption in intermembrane sealing appeared to be at the root of the defects observed in cadherin-deficient epidermis. It is tempting to speculate that the early perturbations in AJ-cortical actin cytoskeleton might alter the stability of the underlying membrane, which in turn could compromise overall cellular architecture. Alterations in actin dynamics may also be responsible for the failure of cadherin-deficient 1^0MK to assemble intercellular junctions *de novo*.

The loss of both Ecad and Pcad unveiled defects in intercellular adhesion, survival and epidermal integrity that were not present in skin lacking only one of these cadherins. To some extent, these newfound defects resembled those of α-catenin-deficient skin (6), and it was notable that cortical α-catenin was selectively diminished only when both cadherins were missing. That said, the Pcad/Ecad and α-catenin mutant mice differed in whether they localized cadherin-β-catenin complexes at cell borders, and this difference may account for other distinctions in the observed phenotypes.

Thus, although epidermal hyperthickening was observed in both mutants, the hyperthickening arising from cadherin inhibition was not accompanied by significant changes in proliferation or MAPK activation. Additionally, while intercellular adhesion was compromised in both cases, only the α-*catenin* cKO mice displayed an inflammatory cell infiltrate and enhanced epidermal NF-κB activation (12). Together, our *in vivo* studies suggest that proliferative and proinflammatory defects arising from loss of α-catenin within epidermis are independent of cadherin-mediated adhesion and provide strong support for our prior *in vitro* analyses (6, 12).

In summary, we have identified new roles for epidermal cadherins in mediating effective intercellular junction formation in keratinocytes *in vitro* and in maintaining epidermal tissue

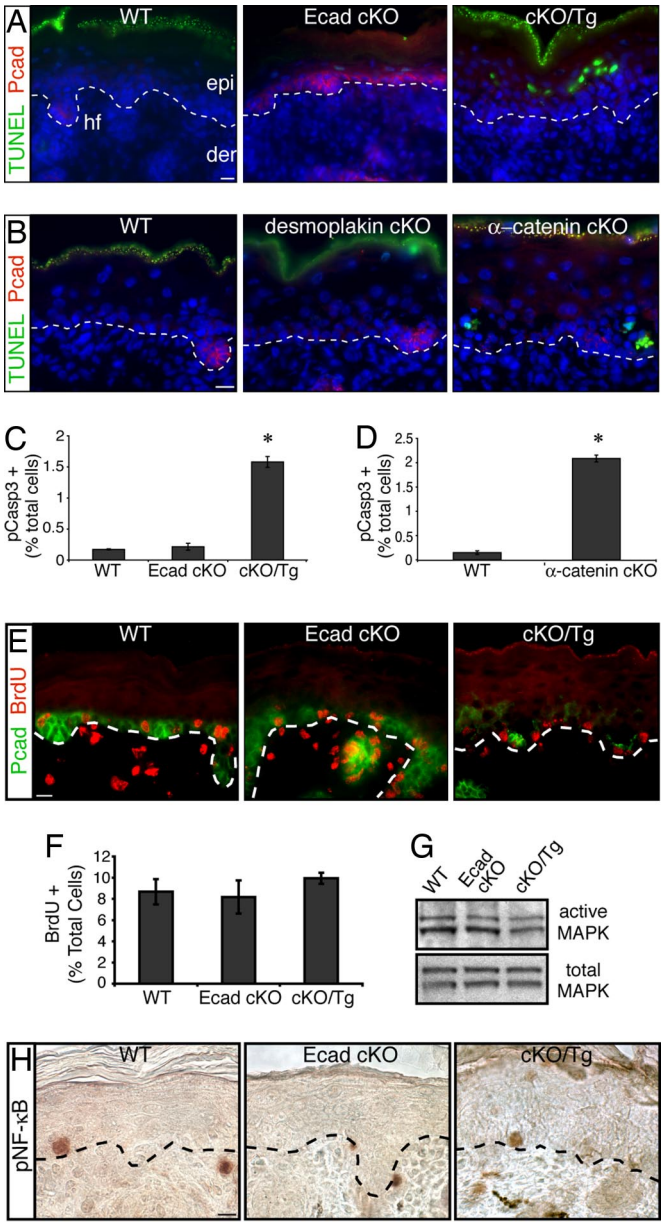

Fig. 6. *In vivo* cadherin and catenin inhibition results in an increase in epidermal apoptosis, yet loss of epidermal cadherins does not perturb proliferative and inflammatory responses. (*A* and *B*) P0 backskins and E18.5 embryos, respectively, were processed for labeling of fragmented DNA via TUNEL. (*C* and *D*) Quantification of active-caspase 3 (pCasp3) immunofluorescence of indicated littermate samples. Data were collected from two independently processed sets of animals. Results are shown as percent anti-pCasp3 immunoreactive cells of the total epidermal cells counted. Asterisks denote significant difference from WT cells determined by *t* test: (*C*): $P < 1 \times 10^{-5}$; (*D*): $P < 1 \times 10^{-10}$. Error bars represent SD. (*E* and *H*) P0 backskins were processed for indirect immunofluorescence and immunohistochemistry with indicated Abs. (*F*) Quantification of BrdU-labeling experiments. P0 mice were injected s.c. with 50 μg/g wt BrdU and killed 2 h. later. Data were collected from two independently labeled sets of animals. Results are shown as percent BrdU-labeled cells of the total epidermal cells counted. Error bars represent SD. (*G*) Total P0 epidermal lysates were processed for immunoblot analysis with indicated Abs. (Scale bars: 10 μm.)

integrity *in vivo*. Although further studies will be necessary to fully appreciate the functional parallels between cadherins and α-catenin, our results suggest that these AJ components function coordinately in mediating keratinocyte adhesion, yet differ in their ability to influence proliferative and inflammatory responses in skin. These observations are interesting in light of the many cancers involving alterations in the expression of both cadherins and catenins and suggest that the loss of one may not functionally equate to the loss of the other.

Materials and Methods

shRNA, Constructs and Generation of Mice. *Pcad* shRNAs were designed by J. Silva and cloned into pMLP vector (J. Silva, Cold Spring Harbor, Cold Spring Harbor, NY) containing microRNA 30 adaptor sequences (see *SI Materials and Methods*) (26). Ecad-GFP (A. Vaezi and E. Fuchs, Rockefeller University, New York, NY) was PCR amplified and cloned into pMSCVpuro (Clontech). Pcad cDNA (M. Takiechi, RIKEN, Kobe, Japan) was amplified by PCR, cloned into pEGFP-N1 (Invitrogen) and subsequently subcloned into pMSCVpuro. 4 bp changes were introduced in Pcad cDNA to generate silent mutations within the region targeted by PcadRNAi through Quikchange site directed mutagenesis kit (Stratagene). This was PCR amplified and cloned into a modified retroviral vector pMSCVhyg (Clontech) expressing the cDNA of cherry fluorescent protein (R. Tsien, University of California at San Diego, La Jolla, CA) to generate a C-terminal tagged mutant Pcad-cherry protein. All constructs were confirmed by DNA sequencing.

Generation of mice expressing *K14-Pcad* shRNA are described in *SI Materials and Methods*. Three independent PcadRNAi Tg lines were maintained and mated to *Ecad* cKO mice (10) to generate epidermal-specific cadherin-deficient mice. K14-Cre Tg (27), K14-GFPactin Tg (27, 28), *α-catenin* cKO (6), *desmoplakin* cKO (22) and *P-cadherin*$^{-/-}$ (7) mice have been previously described.

Tissue Processing and Analyses. Tissues were frozen, fixed, sectioned and subjected to immunofluorescence (10). Additional Abs: P-cadherin (1:300; R&D systems), N-cadherin (Invitrogen), pan-cadherin (Sigma), l/s-afadin (Sigma), pan-desmoglein (1:300; Fitzgerald), desmocollin 2 (1:300; Fitzgerald), occludin (Invitrogen), claudin 1 (Invitrogen), ZO-1 (Invitrogen), Par3 (Upstate), aPKCλ (Santa Cruz), Scribble (Santa Cruz), RFP (MBL International), phosphohistone H3 (1:300; Millipore), BrdU (1:300; Abcam), active caspase 3 (R&D systems), CD3 (Chemicon), CD11b (1:25; BD Biosciences), active MAPK (Sigma), phospho-NF-κB (Cell Signaling), α-tubulin (1:1,000; Serotec). Unless otherwise stated, 1^0Abs were used at 1:100. 2^0Abs and dilutions were: Alexa Fluor 488 (1:1,000; Invitrogen), rhodamine RedX and cy5 (1:200; Jackson Labs). For immunohistochemistry, biotin-conjugated 2^0Abs (1:100) were used and developed using the Vectastain ABC kit and DAB substrate (Vector Labs). Additional reagents were TRITC/Alexa Fluor 647-Phalloidin (Sigma/Invitrogen), ApopTag fluorescein direct in situ apoptosis detection kit (Chemicon), and 4′6′-diamidino-2-phenylindole (DAPI) to label nuclei.

For transmission EM, tissues were fixed, processed and visualized as described (29).

ACKNOWLEDGMENTS. We thank M. Takeichi (RIKEN) for reagents; G. Radice (University of Pennsylvania) for *P-cadherin*$^{-/-}$ mice; J. Silva (Cold Spring Harbor Laboratories) for RNAi design and reagents; R. Tsien (University of California at San Diego) for reagents; L. Polak and Laboratory Animal Research Center staff for expert care and breeding of mice; M. Perez-Moreno and B. Short for experimental assistance and other members of the Fuchs Lab for advice and critical reading of the manuscript. Mice were housed and bred in the LARC ALAAC-accredited animal facility at The Rockefeller University. C.T. is an MD/PhD student supported by NIH MSTP grant GM07739 and partially by NRSA training grant CA09673. E.F. is an Investigator of the Howard Hughes Medical Institute. This work was supported by National Institutes of Health Grant R01-AR27883 (to E.F.).

1. Gumbiner BM (2005) Regulation of cadherin-mediated adhesion in morphogenesis. *Nat Rev Mol Cell Biol* 6:622–634.
2. Nose A, Nagafuchi A, Takeichi M (1988) Expressed recombinant cadherins mediate cell sorting in model systems. *Cell* 54:993–1001.
3. Patel SD, *et al.* (2006) Type II cadherin ectodomain structures: Implications for classical cadherin specificity. *Cell* 124:1255–1268.
4. Halbleib JM, Nelson WJ (2006) Cadherins in development: Cell adhesion, sorting, and tissue morphogenesis. *Genes Dev* 20:3199–3214.
5. Perez-Moreno M, *et al.* (2006) p120-catenin mediates inflammatory responses in the skin. *Cell* 124:631–644.
6. Vasioukhin V, Bauer C, Degenstein L, Wise B, Fuchs E (2001) Hyperproliferation and defects in epithelial polarity upon conditional ablation of alpha-catenin in skin. *Cell* 104:605–617.
7. Radice GL, Ferreira *et al.* (1997) Precocious mammary gland development in P-cadherin-deficient mice. *J Cell Biol* 139:1025–1032.
8. Huelsken J, Vogel R, Erdmann B, Cotsarelis G, Birchmeier W (2001) beta-Catenin controls hair follicle morphogenesis and stem cell differentiation in the skin. *Cell* 105:533–545.
9. Young P, *et al.* (2003) E-cadherin controls adherens junctions in the epidermis and the renewal of hair follicles. *EMBO J* 22:5723–5733.
10. Tinkle CL, Lechler T, Pasolli HA, Fuchs E (2004) Conditional targeting of E-cadherin in skin: Insights into hyperproliferative and degenerative responses. *Proc Natl Acad Sci USA* 101:552–557.
11. Tunggal JA, *et al.* (2005) E-cadherin is essential for in vivo epidermal barrier function by regulating tight junctions. *EMBO J* 24:1146–1156.
12. Kobielak A, Fuchs E (2006) Links between alpha-catenin, NF-kappaB, and squamous cell carcinoma in skin. *Proc Natl Acad Sci USA* 103:2322–2327.
13. Bierkamp C, McLaughlin KJ, Schwarz H, Huber O, Kemler R (1996) Embryonic heart and skin defects in mice lacking plakoglobin. *Dev Biol* 180:780–785.
14. Hatta M, *et al.* (1991) Genomic organization and chromosomal mapping of the mouse P-cadherin gene. *Nucleic Acids Res* 19:4437–4441.
15. Hardy MH, Vielkind U (1996) Changing patterns of cell adhesion molecules during mouse pelage hair follicle development. 1. Follicle morphogenesis in wild-type mice. *Acta Anat (Basel)* 157:169–182.
16. Jamora C, DasGupta R, Kocieniewski P, Fuchs E (2003) Links between signal transduction, transcription and adhesion in epithelial bud development. *Nature* 422:317–322.
17. Furuse M, *et al.* (2002) Claudin-based tight junctions are crucial for the mammalian epidermal barrier: A lesson from claudin-1-deficient mice. *J Cell Biol* 156:1099–1111.
18. Nelson WJ (2003) Adaptation of core mechanisms to generate cell polarity. *Nature* 422:766–774.
19. Qin Y, Capaldo C, Gumbiner BM, Macara IG (2005) The mammalian Scribble polarity protein regulates epithelial cell adhesion and migration through E-cadherin. *J Cell Biol* 171:1061–1071.
20. Vasioukhin V, Bauer C, Yin M, Fuchs E (2000) Directed actin polymerization is the driving force for epithelial cell-cell adhesion. *Cell* 100:209–219.
21. Boussadia O, Kutsch S, Hierholzer A, Delmas V, Kemler R (2002) E-cadherin is a survival factor for the lactating mouse mammary gland. *Mech Dev* 115:53–62.
22. Vasioukhin V, Bowers E, Bauer C, Degenstein L, Fuchs E (2001) Desmoplakin is essential in epidermal sheet formation. *Nat Cell Biol* 3:1076–1085.
23. Fuchs E (2007) Scratching the surface of skin development. *Nature* 445:834–842.
24. Gumbiner B, Stevenson B, Grimaldi A (1988) The role of the cell adhesion molecule uvomorulin in the formation and maintenance of the epithelial junctional complex. *J Cell Biol* 107:1575–1587.
25. Capaldo CT, Macara IG (2007) Depletion of E-cadherin disrupts establishment but not maintenance of cell junctions in Madin-Darby canine kidney epithelial cells. *Mol Biol Cell* 18:189–200.
26. Silva JM, *et al.* (2005) Second-generation shRNA libraries covering the mouse and human genomes. *Nat Genet* 37:1281–1288.
27. Vasioukhin V, Degenstein L, Wise B, Fuchs E (1999) The magical touch: Genome targeting in epidermal stem cells induced by tamoxifen application to mouse skin. *Proc Natl Acad Sci USA* 96:8551–8556.
28. Vaezi A, Bauer C, Vasioukhin V, Fuchs E (2002) Actin cable dynamics and Rho/Rock orchestrate a polarized cytoskeletal architecture in the early steps of assembling a stratified epithelium. *Dev Cell* 3:367–381.
29. Alonso L, *et al.* (2005) Sgk3 links growth factor signaling to maintenance of progenitor cells in the hair follicle. *J Cell Biol* 170:559–570.